

Comparison of Aster Thermal Bands and feature Identification Using Advance Spectroscopic Techniques

Krishnendu Banerjee¹, Surajit Panda¹, Dr. Manish Kumar Jain², Dr. A.T Jeyaseelan³, and Ratnesh Kr. Sharma¹

¹Jharkhand Space Applications Center,
Dept. of Information Technology, Govt. of Jharkhand,
Ranchi- 834004, Jharkhand, India

²Dept. of Environmental Science & Engineering,
Indian School of Mines (ISM),
Dhanbad-826004, Jharkhand, India

³Regional Remote Sensing Centre West ,
NRSC, ISRO,
Jodhpur - 342003 Rajasthan, India

Copyright © 2014 ISSR Journals. This is an open access article distributed under the *Creative Commons Attribution License*, which permits unrestricted use, distribution, and reproduction in any medium, provided the original work is properly cited.

ABSTRACT: Land surface temperature (LST) is important factor in surface feature mapping, analysis, and estimation of emissivity and heat balance studies. The knowledge of surface temperature is important for various applications in Remote sensing field. Feature mapping and analysis can be done according to their emissivity and brightness temperature. In this investigation an attempt has been made to estimate surface temperature from ASTER and to use the relationship between aster thermal bands for feature mapping. ASTER has 5 thermal bands (wave length ranging from 8.125 μ m to 11.65 μ m) and these are used in comparison. ASTER thermal bands have been used to convert digital numbers to exoatmospheric radiance using published ASTER user manual gains and offsets. The exoatmospheric radiance is then converted to surface radiance by applying the Emissivity Normalization method, assuming the emissivity of the Investigation area is constant (0.96, the emissivity of urban areas).The surface temperature is then extracted from the surface radiance, based on ASTER images of May 2007. The extracted temperature data were compared to individual ASTER temperature bands. A positive correlation has been found from this comparison.

KEYWORDS: LST (Land surface temperature), TOA (Top of the atmosphere)

1 INTRODUCTION

The measured radiance from the earth surface in the thermal infrared region is a function of both emissivity and temperature information. Emissivity calculations and subsequent estimation of land surface temperature (LST) using ASTER (TIR) bands have opened up new possibilities for satellite based lithological mapping. Emissivity is controlled by the composition of the surface rock and is often used for constituent/lithological mapping. In this context, silicate minerals play important roles, as emissivity characteristics of silicate minerals are found to be useful indicators of lithology. In the present study, the term 'relative emissivity / emittance' is more relevant than 'absolute emissivity', as it is related to measurement of natural surface rather than ideal specimen. LST is known to be one of the key diagnostic parameters of the physical processes of land surface, involving both surface and subsurface geology (Becker and Li, 1990). LST is controlled by surface energy balance, atmospheric condition, and thermal properties of surface and subsurface formation. Land surface temperature can provide important information about the surface physical properties and climate which plays a role in many environmental processes (Dousset & Gourmelon 2003; Weng, Lu & Schubring 2004). The surface temperature is a main indicator of the

surface energy balance of the Earth and it is used as input data in climate change models, agro-meteorological or hydrological models. Surface temperature can also be used to forecast the soil freezing, to analyse heat islands in urban areas, to decide the optimal timing of agricultural activities, to study volcanoes and geothermal activities, to detect fires, and the exploration of natural resources.

2 AIM AND OBJECTIVE OF THE STUDY

- Calculate Emissivity ASTER thermal bands.
- Calculate surface temperature of ASTER thermal bands.
- Generate Band statistics of ASTER thermal bands.
- Feature identification by using ASTER thermal bands.

3 INVESTIGATION AREA

In the present Investigation, the main Investigation area is in East Singhbhum district and some part of Investigation area covers West Bengal and Odisha State. The complete Aster scene covers or 3600 square kilometre. The Investigation area, lies between $86^{\circ}41'52.22''\text{E}$ to $86^{\circ}13'39.43''\text{E}$ and $22^{\circ}13'58.27''\text{N}$ to $22^{\circ}52'28.52''\text{N}$. It has varying elevation of 10.425–644.370 meters above sea level (ASTER DEM 2007). ASTERL1b data was used in this Investigation. The multi data sets were acquired on Jan152007. They consist of Band 5, Thermal Infrared data, and were obtained from the Jharkhand Space Application Centre in HDF format.

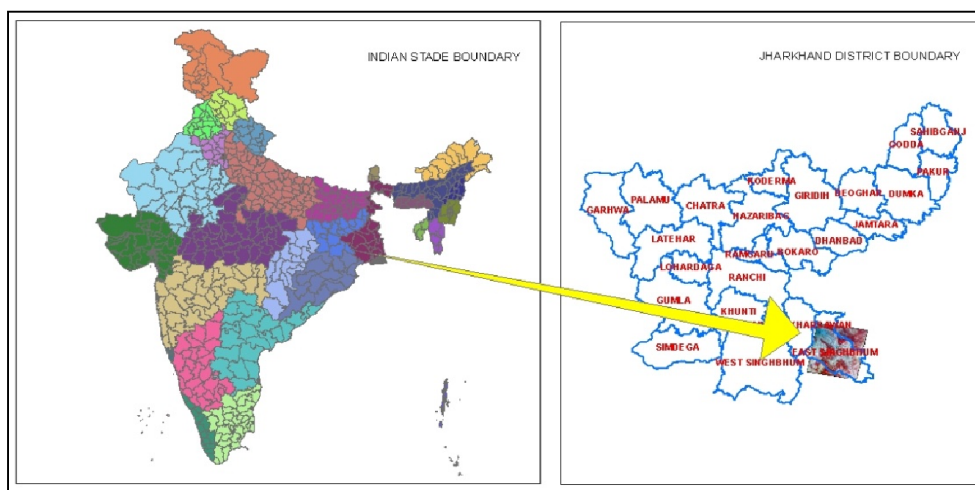


Fig: 1 Location map of the study area

4 METHODOLOGY

The relationship of Bands in infrared region allows the calculation of the surface temperature of the scene thermal channels. The infrared radiance measured from a satellite can be converted to surface radiance by applying the reference channel method. The surface radiance is then converted to surface temperature. The methodology followed is schematically shown in Figure 3. Thermal bands were processed using ENVI 4.7 (Fig: 2)

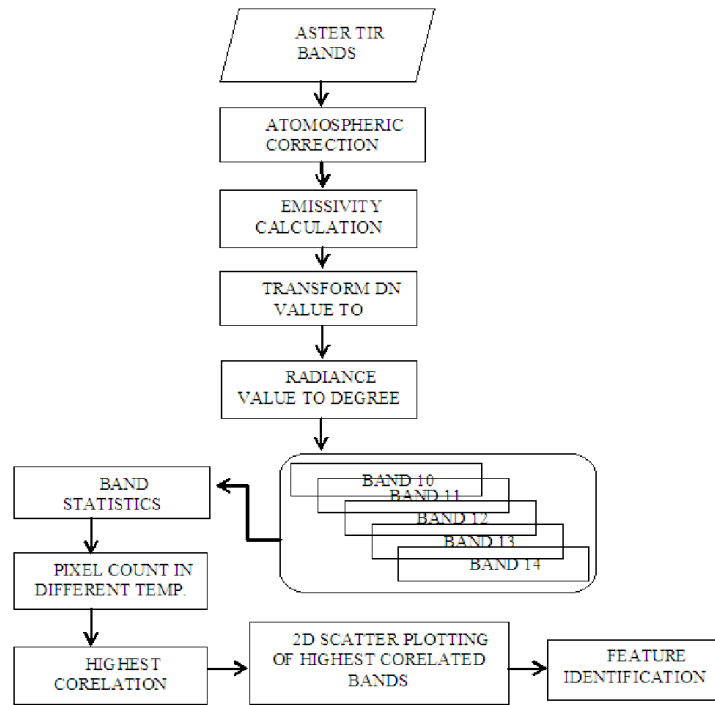


Fig: 2 Detail flow Diagram of Methodology

5 DETAIL PROCEDURE OF FUNCTIONS USED

5.1 DN TO SPECTRAL RADIANCE

Data used here, as an example, is ASTER L1B data (version 3.0), radiometrically Re-calibrated digital numbers, 8bit (1-255) for visible and near-infrared bands and 12 bit (1-4095) for thermal infrared (TIR) bands (table: 1). Dn to spectral radiance is converted by using eq 1.

$$L_{rad,j} = (DN_j - 1) \times UCC_j \quad (\text{eq. 1})$$

Where, $L_{rad, j}$ is ASTER spectral radiance at the sensor's aperture measured in a wavelength j ; j is the ASTER band number; DN_j is the unitless DN values for an individual band j ; UCC_j is the Unit Conversion Coefficient ($W\ m^{-2}sr^{-1}\ \mu m^{-1}$) from ASTER Users Handbook.

Table 1: Calculated Unit Conversion Coefficients

BAND#	Maximum Radiance (W m ⁻² sr ⁻¹ μm ⁻¹)			
	High gain	Normal Gain	Low Gain 1	Low gain 2
1	0.676	1.688	2.25	N/A
2	0.708	1.415	1.89	
3N	0.423	0.862	1.15	
3B	0.423	0.862	1.15	
4	0.1087	0.2174	0.29	0.29
5	0.0348	0.0696	0.0925	0.409
6	0.0313	0.0625	0.083	0.39
7	0.0299	0.0597	0.0795	0.332
8	0.0209	0.0417	0.0556	0.245
9	0.0159	0.0318	0.0424	0.265
10	N/A	0.006822	N/A	N/A
11		0.00678		
12		0.00659		
13		0.005693		
14		0.005225		

5.2 SPECTRAL RADIANCE TO TOA (TOP OF THE ATMOSPHERE) REFLECTANCE

ASTER at-sensor reflectance (ρ_{TOA} also called as planetary reflectance or apparent reflectance or TOA reflectance) for a specific band j is calculated using the standard Landsat equation (eq 2) as:

$$\rho_{TOA,\lambda} = \frac{\pi \cdot L_{rad,\lambda} \cdot d^2}{E_{SUN,\lambda} \cdot \cos(\theta_s)} \tag{eq. 2}$$

Where, ρ_{TOA} is Unit less planetary reflectance, L_{rad} is Spectral radiance at the sensor's aperture, D is Earth% Sun distance in astronomical units from an Excel file which is calculated using the below EXCEL equation (Achard and D’Souza 1994; Eva and Lambin, 1998) or interpolated from values listed in (Table 2), E_{sun} is mean solar exoatmospheric irradiances, λ is wavelength, corresponds to the band number j, θ_s is solar zenith angle in degrees (zenith angle = 90– solar elevation angle), which is found in the ASTER header file.

5.3 TOA REFLECTANCE TO SURFACE REFLECTANCE

Table 2: Earth-Sun Distance in Astronomical Units

Days of Year	Distance								
1	0.98331	74	0.99446	152	1.01403	227	1.01281	305	0.99253
15	0.98365	91	0.99926	166	1.01577	242	1.00969	319	0.98916
32	0.98536	106	1.00353	182	1.01667	258	1.00566	335	0.98608
46	0.98774	121	1.00756	196	1.01646	274	1.00119	349	0.98426
60	0.99084	135	1.01087	213	1.01497	288	0.99718	365	0.98333

Surface reflectance is calculated using empirical methods when ground truth is available by correlating the field measured surface reflectance with synchronous pixel value, or radiative transfer models such as MODTRAN , 6S (Second Simulation of the Satellite Signal in the Solar Spectrum, Vermote, et al., 1997), etc.

It is recommended to use surface reflectance products for quantitative remote sensing analysis, however, TOA reflectance based outcome is also acceptable due to the fact that land surface reflectance retrieval is complicated.

5.4 TEMPERATURE CALCULATION

5.4.1 DNS TO RADIANCE

Refer to Part1 Step1 to convert DNS to radiance for thermal bands. There is no difference between converting DNS to radiance of thermal or optical data.

5.4.2 SPECTRAL RADIANCE TO TOA BRIGHTNESS TEMPERATURE

Planck’s Radiance Function (eq 3)

$$B_{\lambda}(T) = \frac{C_1}{\lambda^5 (e^{\frac{C_2}{\lambda T}} - 1)} \tag{eq. 3}$$

Where, C_1 is $1.19104356 \times 10^{-16} \text{ W m}^2$; C_2 is $1.43876869 \times 10^{-2} \text{ m K}$

In the absence of atmospheric effects, T of a ground object can be theoretically determined by inverting the Planck’s function as follows (eq 4):

$$T = \frac{C_2}{\lambda \cdot \ln \left[\frac{C_1}{\lambda^5 B_{\lambda}(T)} + 1 \right]} \tag{eq. 4}$$

This equation can be reformed (eq 5) as

$$T = \frac{\frac{C_2}{\lambda}}{\ln \left[\frac{C_1}{\lambda^5} \frac{1}{B_{\lambda}(T)} + 1 \right]} \tag{eq. 5}$$

Let K_1 is C_1/λ^5 , and K_2 is C_2/λ , and satellite measured radiant intensity $B_{\lambda}(T)$ is L_{λ} , then above mentioned equation is collapsed into an equation similar to the one used to calculate brightness temperature from Landsat TM image. The equation (eq 6) is.

$$T = \frac{K_2}{\ln \left(\frac{K_1}{L_{\lambda}} + 1 \right)} \tag{eq. 6}$$

Therefore, K_1 and K_2 become a coefficient determined by effective wavelength of a satellite sensor. For example, effective wavelength of ASTER band 10, $\lambda=8.291\mu\text{m} = 8.291 \times 10^{-6} \text{ m}$, we can have $K_1 = C_1/\lambda^5 = 1.19104356 \times 10^{-16} \text{ W m}^{-2} / (8.291 \times 10^{-6} \text{ m})^5 = 3040136402 \text{ W m}^{-2} \mu\text{m}^{-1} = 3040.136402 \text{ W m}^{-2} \mu\text{m}^{-1}$ $K_2 = C_2/\lambda = 1.43876869 \times 10^{-2} \text{ m K} / 8.291 \times 10^{-6} \text{ m} = 1735.337945 \text{ K}$. The values of other bands are given in (Table 3).

Table 3: ASTER thermal bands (referenced ASTER L1B Manual Ver.3.0)

Bands	Bandpass	Effective	UCC	K1(W m ⁻² μm ⁻¹)	K (K)
10	(μm)	Wavelength (μm)	0.006882	3040.136402	1735.33795
11	8.475-8.825	8.634	0.00678	2482.375199	1666.39876
12	8.925-9.275	9.075	0.00659	1935.060183	1585.42004
13	10.25-10.95	10.657	0.005693	866.468575	1350.06915
14	10.95-11.65	11.318	0.005225	641.326517	1271.22167

6 RESULT AND DISCUSSION

The temperature of successive band has been calculated from the reference channel method. The highest temperature of successive thermal bands is found 316.75°K and lowest is 288.36°K. The mean value is 302.66°K. All the bands has the same range of temperature but the power of discrimination of objects is varies as their wave length changes in different bands. The spectral wavelength of band 10 is (8.12-8.47µm). The wavelengths increase in the successive bands and range to (10.95-11.65µm) at band 14. The temperature map and the band statistics has been calculated every individual band of ASTER. (Fig: 3)

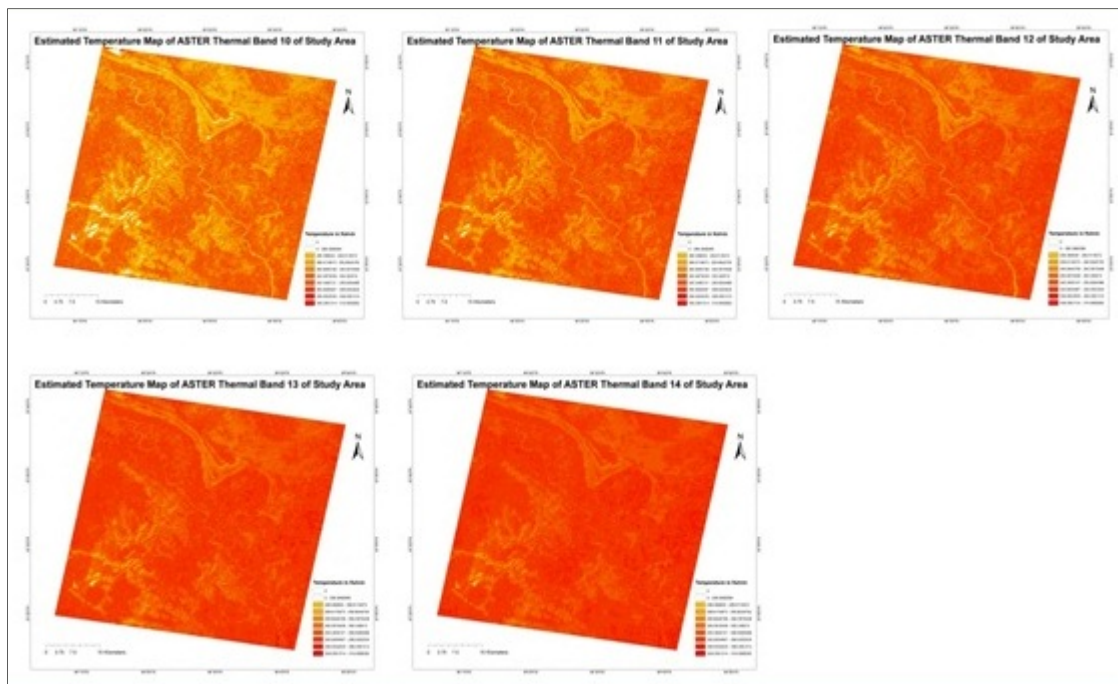


Fig: 3 Temperature maps of different thermal bands (ASTER)

The temperature variation of different channels varies between 284°K to 316°K. Pixel count has been taken in each temperature range. The concentration of pixel count is maximum 287-302°K in the study area. The image has been taken in day time and the study area is belongs to chhotanagpur platue region so the temperature variation is very high.

While comparing the pixel count at same temperature range of different thermal channels, it is found that the maximum pixel count or pick temperature is found in band 10 at 292°K (129185 pixels). A positive relation is found in wavelength and temperature. Band 10 and Band 11 is found mostly co-related bands in temperature estimation. The discrimination power of different surface features is found best in Band 10 and Band 11.

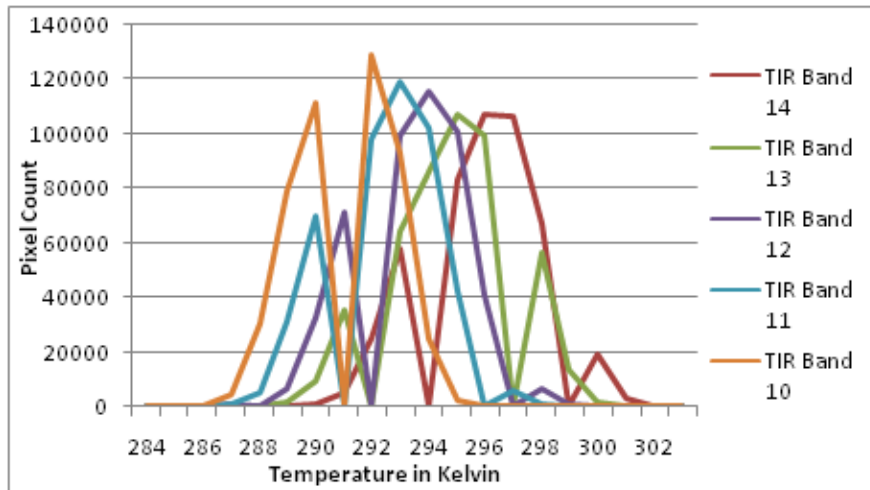


Fig: 4 Statistical comparisons of different temperature channel (ASTER)

While comparing the mostly co-related bands (10, 11) it shows the positive co relation. A different physical characteristic is found in different physical objects. Like water bodies heats quickly and release heat slowly in daytime and absorbs the most part of inferred region. Green vegetation reflects the most part of inferred region. So a lowest co-relation is found in the case of wet lands (red colour shows wet lands). A moderate co-relation is found in the case of vegetation (green coloured shows vegetation).The fellow land shows strong co-relation in the scatter plot (brown colour shows bare land) in Fig: 5.

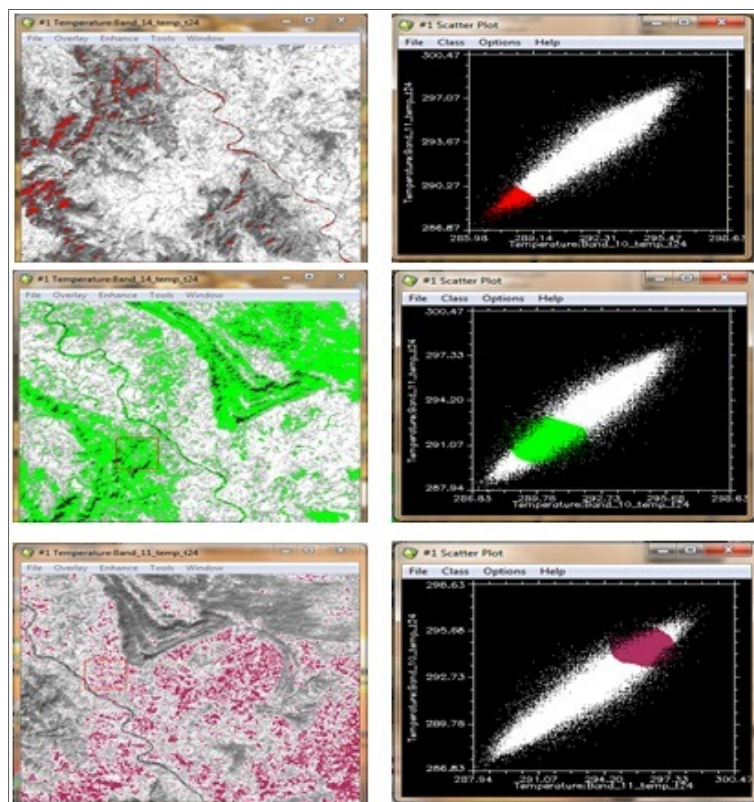


Fig: 5 Feature identification using temperature channel combination

7 CONCLUSION

The Present study shows the effective utilization of thermal remote sensing data for thermal mapping and detection of thermal anomalies. This study was carried out with the primary objective of finding the suitability of ASTER thermal bands data in providing land surface temperatures as well as the new dimension in feature identification. The primary goal is to find co-relation of ASTER thermal bands in LST (Land Surface Temperature) calculation. The effective wavelength of TIR bands are used for analysis. There are many other methods available for LST calculation like emissivity normalization but reference channel method is found the most effective method as it calculates the LST of individual bands assuming the constant emissivity value of .96. Feature identification should be applied in large areas or in large scale. The comparison of LST of different bands is found most helpful method in feature identification then visual image interpretation technique. But it limits the feature identification in small scale. Overall result of feature identification is found helpful for geological or geomorphological studies.

REFERENCES

- [1] Abduwasit Ghulam (2009). How to calculate reflectance and temperature using ASTER data. Center for Environmental Sciences at Saint Louis University.
- [2] BECKER, F. (1987) Impact of spectral emissivity on the measurement of land surface temperatures from a satellite, Received: 3 Mar 1987, Accepted: 23 May 1987, Published online: 07 May 2007.
- [3] D.W.J. Stein, S.G. Beaven et al. "Anomaly Detection from Hyperspectral Imagery", and Date of Publication: Jan 2002, **ISSN: 1053-5888**.
- [4] GILLESPIE, KAHLE A.B.et.al (1998) A temperature and emissivity separation algorithm for Advanced Space borne Thermal Emission and Reflection Radiometer (ASTER) images. Date of Publication: Jul 1998, **ISSN: 0196-2892**.
- [5] Hook S J, Vaughan R G et al. (2007) Absolute radiometric in-flight validation of Midand Thermal Infrared data from ASTER and MODIS using the Lake Tahoe CA/NV, USA automated validation site. Date of Publication: June 2007, **ISSN: 0196-2892**.
- [6] Jacob F, Petitcolin F et al.(2004) Comparison of land surface emissivity and radiometric temperature derived from MODIS and ASTER sensors. Received 12 August 2003; received in revised form 24 November 2003; accepted 28 November 2003.
- [7] Jensen J.R, 2000, "Remote sensing of Environment-an Earth Resource Perspective" Published by Pearson Education.
- [8] R.J. Muirhead, (1982): "Aspects of Multivariate Statistical Theory". Copyright 1987. Online ISBN : 9 8-94-017-0653-7, pp 277-288
- [9] S. Rajendran, S. Aravindan et al. (2009), "Hyperspectral Remote sensing and Spectral Signature Application". pp 200-203
- [10] Sobrino J A, El Kharraz J and Li Z-L 2003 Surface temperature and water vapour retrieval from MODIS data. Received 14 May 2002; in final form 10 February 2003.